RL-TR-95-20
Final Technical Report
February 1995

QUANTUM CYLINDER FIBER LIGHT AMPLIFIER

Syracuse University

Philipp Kornreich

DTIC
SELECTED
MAY 1 5 1995
G

APPROVED FOR PUBLIC RELEASE; DISTRIBUTION UNLIMITED.

19950512 111

DTIC QUALITY INSPECTED 5

Rome Laboratory
Air Force Materiel Command
Griffiss Air Force Base, New York

This report has been reviewed by the Rome Laboratory Public Affairs Office (PA) and is releasable to the National Technical Information Service (NTIS). At NTIS it will be releasable to the general public, including foreign nations.

RL-TR-95-20 has been reviewed and is approved for publication.

APPROVED:

JOHN L. STACY
Project Engineer

FOR THE COMMANDER:

DONALD W. HANSON
Director of Surveillance & Photonics

If your address has changed or if you wish to be removed from the Rome Laboratory mailing list, or if the addressee is no longer employed by your organization, please notify RL (OCPA) Griffiss AFB NY 13441. This will assist us in maintaining a current mailing list.

Do not return copies of this report unless contractual obligations or notices on a specific document require that it be returned.

REPORT DOCUMENTATION PAGE

Public reporting burden for this collection of information is estimated to average 1 hour per response, including the time for reviewing instructions, searching existing data sources, gathering and maintaining the data needed, and completing and reviewing the collection of information. Send comments regarding this burden estimate or any other aspect of this collection of information, including suggestions for reducing this burden, to Washington Headquarters Services, Directorate for Information Operations and Reports, 1215 Jefferson Davis Highway, Suite 1204, Arlington, VA 22202-4302, and to the Office of Management and Budget, Paperwork Reduction Project (0704-0188), Washington, DC 20503.

1. AGENCY USE ONLY (Leave Blank)	2. REPORT DATE February 1995	3. REPORT TYPE AND DATES COVERED Final Mar 93 – Mar 94

4. TITLE AND SUBTITLE

QUANTUM CYLINDER FIBER LIGHT AMPLIFIER

5. FUNDING NUMBERS
C – F30602-93-C-0019
PE – 62702F
PR – 4600
TA – P1
WU – PK

6. AUTHOR(S)

Philipp Kornreich

7. PERFORMING ORGANIZATION NAME(S) AND ADDRESS(ES)

Syracuse University
113 Bowne Hall
Syracuse NY 13244-1200

8. PERFORMING ORGANIZATION REPORT NUMBER

N/A

9. SPONSORING/MONITORING AGENCY NAME(S) AND ADDRESS(ES)

Rome Laboratory (OCPA)
25 Electronic Pky
Griffiss AFB NY 13441-4515

10. SPONSORING/MONITORING AGENCY REPORT NUMBER

RL-TR-95-20

11. SUPPLEMENTARY NOTES

Rome Laboratory Project Engineer: John L. Stacy/OCPA/(315) 330-2937

12a. DISTRIBUTION/AVAILABILITY STATEMENT

Approved for public release; distribution unlimited.

12b. DISTRIBUTION CODE

13. ABSTRACT (Maximum 200 words)

The objective of this effort was to fabricate and test Quantum Cylinder Fiber Light Amplifiers (QCyFLA). These devices are to be used for optical amplification. During the course of this effort, we were able to fabricate and test devices as planned. Test results were not the same as the theoretical predictions. New devices will be fabricated using a wide gap semiconductor against the glass. This should shift the absorption edge to the predicted wavelength.

14. SUBJECT TERMS

Communications, Fiber optics, Amplification

15. NUMBER OF PAGES 30

16. PRICE CODE

17. SECURITY CLASSIFICATION OF REPORT	18. SECURITY CLASSIFICATION OF THIS PAGE	19. SECURITY CLASSIFICATION OF ABSTRACT	20. LIMITATION OF ABSTRACT
UNCLASSIFIED	UNCLASSIFIED	UNCLASSIFIED	UL

ABSTRACT

We are working on Quantum Cylinder Fiber Light Amplifiers (QCyFLA). We have experimentally demonstrated that CdTe semiconductor films survive the fiber fabrication process. Indeed the quality of the semiconductor increases during the fiber fabrication process. This is usually, during semiconductor device fabrication subsequent steps tend to degrade the results achieved in previous fabrication steps. During this reporting period a multi source vacuum system for depositing multi layer semiconductor films was designed and built. This vacuum system will be capable of depositing $Pb_xCd_{1-x}S$ films that can be used to amplify optical signals at a wavelength of 1.3 µm. A new two floor high fiber fabricating facility was designed and is now in the final stages of fabricating. This facility will allow us to fabricate about 500 m long uniform fibers in each run.

1 CdTe FIBER FABRICATION AND TESTING.

a) Current Fiber Fabrication.

The purpose of this effort to fabricate and test Quantum Cylinder Fiber Light Amplifiers (QCyFLA). These devices are fabricated as follows: The preform is formed by depositing semiconductor films on a glass rod. The glass is inserted into a glass tube. The space between the glass rod and tube is evacuated, and the tube is collapsed unto the rod and semiconductor film by heating the glass tube. A fiber is, subsequently, pulled from this preform.

We have experimentally demonstrated that CdTe semiconductor films survive the fiber fabrication process. CdTe powder was readily available and could readily be vacuum deposited with the metalization system. Also, CdTe melts at 935 °C which is higher than the softening temperature of 650 °C of the glass used in our fibers. We have, also, recently fabricated CdS films that can be used for non linear optical applications.

Indeed, the fist semiconductor fibers that we attempted to fabricate use InSb. Since InSb has a very small effective mass it should display a large quantum size effect. The quantum size effect is not necessary for the QCyFLA operation. However, it is an indication of the quality of the

semiconductor film. We deposited InSb films on glass rods. The films had a dark gray appearance after deposition. However, after the collapsing process the glass rod in the preform was completely clear. The InSb film melted during the process of collapsing of the cladding tube. InSb melts at 350 °C while the collapsing process is performed at 650 °C. We next, tried CdTe which melts at 935 °C. This worked well. The quality of the CdTe semiconductor film increases during the fiber fabrication process. This is usually, during semiconductor device fabrication subsequent steps tend to degrade the results achieved in previous fabrication steps.
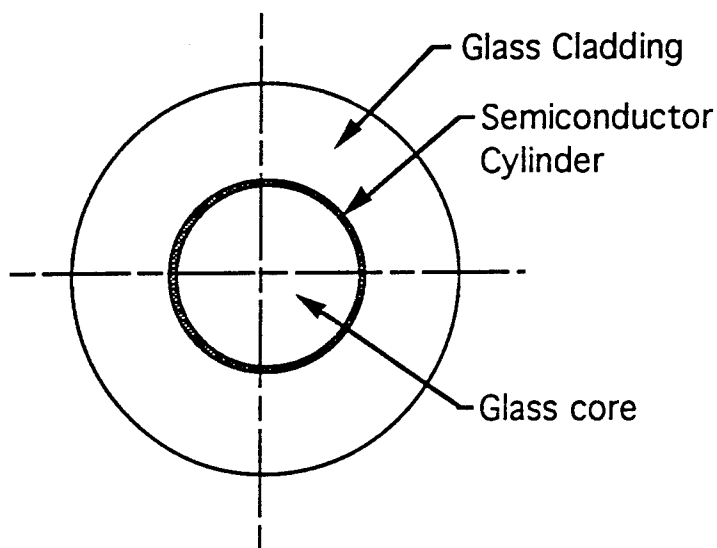

Fig. 1. Typical cross section of a **Q**uantum **Cy**linder **F**iber **L**ight **A**mplifier

During this reporting period we have used our metalization vacuum system to deposit the semiconductor layers. Since there is no facility for heating the glass rods during the vacuum deposition process the deposited films are very metal rich. It appears that during the collapse of the glass tube most of the excess metal evaporates leaving the semiconductor. The preform exhibits an absorption edge at a wavelength of 830 nm, The theoretically predicted absorption edge should be at 794.777 eV, see Fig. 2. Perhaps, this shift in absorption edge can be accounted for by strain? The energy gap of CdTe changes by 1.5×10^{-6} eV per Bar isotropic pressure. There is a difference of 0.0662 eV between the theoretical and measured
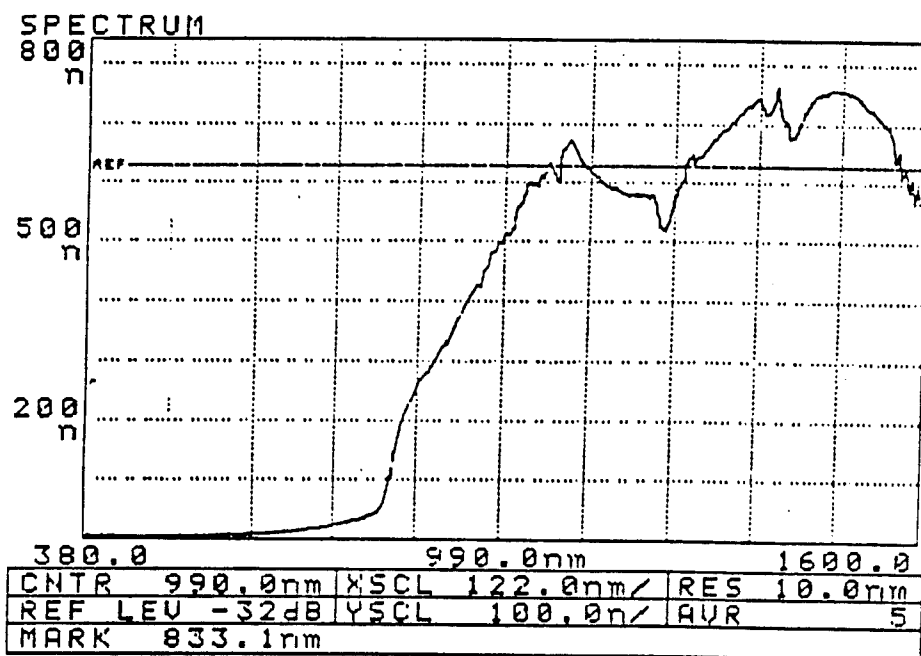
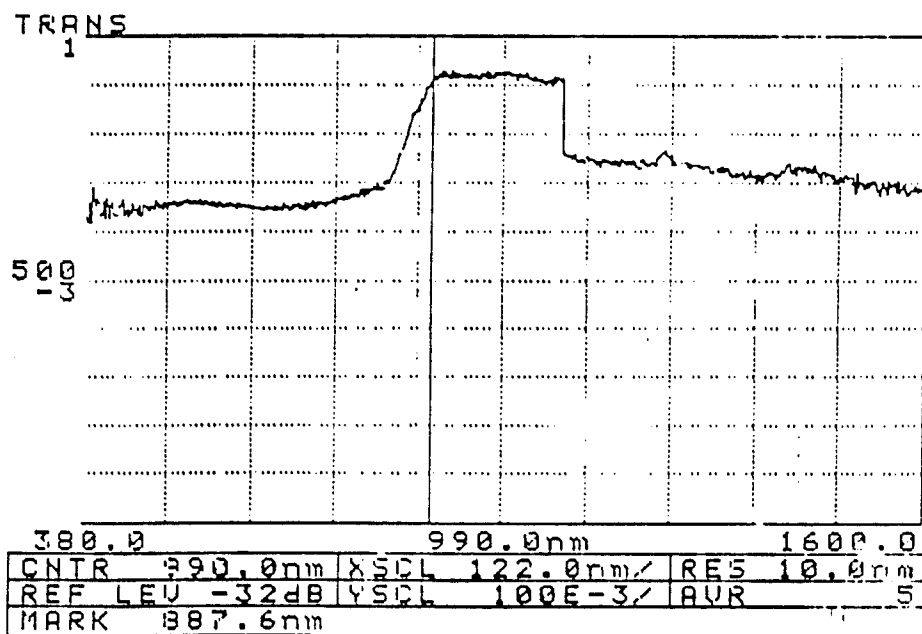**Fig. 2.** Transmission spectrum of CdTe preform. Note the absorption edge at about 830 nm.

Fig. 3. Transmission spectrum of CdTe fiber. Note the absorption edge at about 830 nm. The step at approximately 1075 nm is an artifact of the spectrum analyzer

energy gaps. This corresponds to a pressure of -44134.88 Bar)-4.413488 x 10^9 $\frac{N}{m^2}$). An almost as sharp absorption edge, also, at a wavelength of about 830 nm was observed in the fiber as shown in Fig. 3. We fabricated a number of fibers with identical results.

This was even more apparent in the CdS fibers that we recently fabricated. The CdS films appeared gray after vacuum deposition. Apparently these films were very Cd rich. After the collapsing process the CdS films turned bright yellow, the normal appearance of high purity CdS crystals. Indeed, the preform exhibited a sharp absorption edge at a wavelength of 514 nm. This is in exact agreement with the theoretically predicted absorption edge, see Fig. 4.
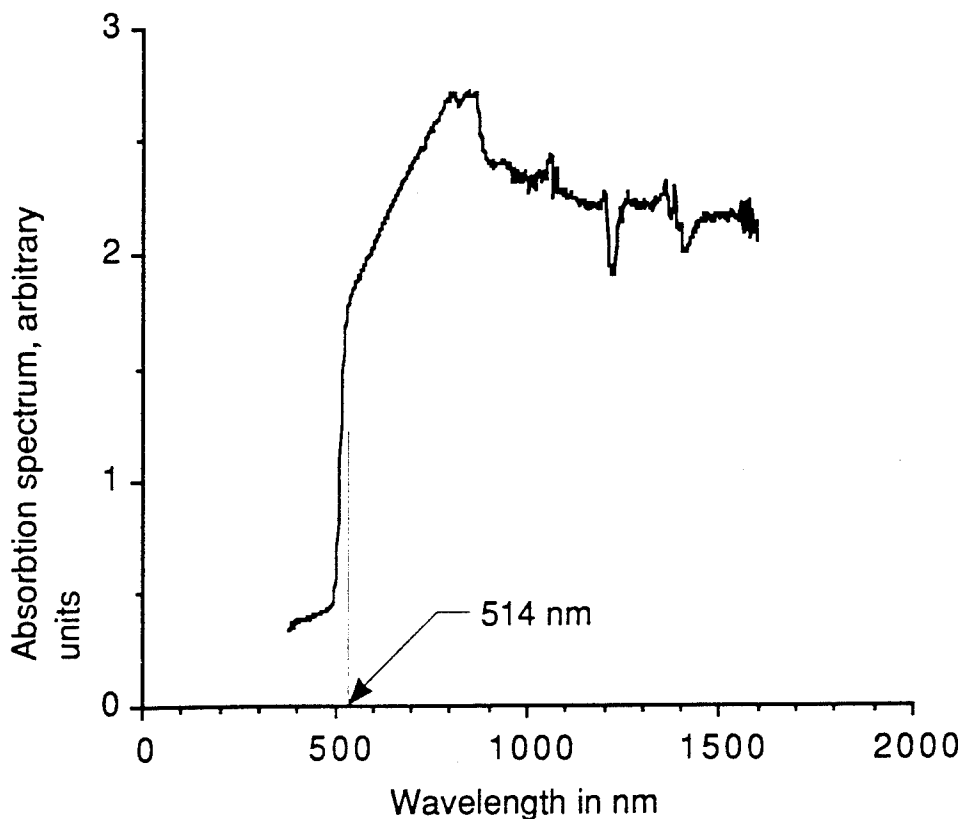

Fig. 4. Transmission spectrum of CdS preform. Note the sharp absorption edge at 514 nm.

The CdTe cylinder fibers were fabricated as follows: The preform is formed by depositing a 0.5 μm CdTe semiconductor films on a 4 mm diameter glass rod. The glass rod surrounded by the CdTe semiconductor

cylinder was inserted into 11 mm inside diameter 14 mm outside diameter a glass tube. The space between the glass rod and tube is evacuated, and the tube is collapsed unto the rod and semiconductor film by heating the glass tube. A fiber is, subsequently, pulled from this preform. The total cross sectional area of the glass tube and glass rod is preserved during the collapsing process. Thus, we predicted that the resulting preform should have a diameter of:

$$d_{preform} = 2\sqrt{\left[\frac{14\ mm}{2}\right]^2 - \left[\frac{11\ mm}{2}\right]^2 + \left[\frac{4\ mm}{2}\right]^2}$$

$$d_{preform} = 9.539\ mm$$

The measured diameter of the preform was 9.52 mm in good agreement with the above predicted value.

During the fiber pulling process the dimensions of all components of the preform shrink proportionally. Thus, since the fiber is approximately 170 μm in diameter the core diameter should be:

$$d_{fiber\ core} = 4\ mm\ \frac{170 \mu m}{9539\ \mu m}$$

$$d_{fiber\ core} = 71.2\ \mu m$$

Assuming the initial thickness of the CdTe film is equal to 0.5 μm one would have 89.1 Å thick CdTe cylinder in the fiber.

Theoretically the fibers should have exhibited a quantum size effect. CdTe has an electron effective mass ratio of 0.11, a hole effective mass ratio of 0.35, and bulk CdTe has an energy gap of 1.56 eV. The quantum size effect should shift the absorption edge to 766.956 nm. However, this seems not to be the case. If one uses the energy gap of 1.494 eV calculate from the measurement of the absorption edge of the preform the quantum size effect in the fiber should shift the absorption edge to 799.6 nm.

There could be several reasons for not being able to observe the quantum size effect. There, probably, are a large number of surface states at the interface of the glass and CdTe film. A similar phenomenon is ob-

served in CdS quantum dots in glass. In future QCyFLAs the number of surface states can be reduced by using wide gap semiconductor layers such as CdS next to the glass and $Pb_xCd_{1-x}S$ active layers sandwiched between the CdS layers. Also, there seem to be semiconductor streaks along the core cladding interface. These streaks would retain properties of the bulk semiconductor.

To date, we have been using the same glass for both the core and cladding. Theoretical calculations as, will be shown below, predict that light should not be guided in the fiber core unless the index of refraction n_1 of the core is greater than the index of refraction n_2 of the cladding ($n_1 > n_2$). We hope to obtain some glass from Corning Inc. where the core has an index of refraction that is 0.2 to 0.4% larger than the index of refraction of the cladding. We, also, have a prescription for changing the index of refraction of the cladding glass by ion exchanging the boron atoms in our Borosilicate glass with sodium atoms from NaOH at 500 °C.

Our present glass contains a large number of enclosures such as sand and air bubbles. One can use a zone refining method for improving the quality of the glass.

b) Data Acquisition Apparatus.

In order to measure the broad band transmission spectrum of the fibers we used a white light source. The experimental arrangement for measuring the transmission spectrum of the fibers is shown in Fig. 5. The apparatus consists of a white light source, followed by a lens. Two microscope objectives are used. to focus the light into the fiber and to retrieve the light from the fiber. There is another lens which focuses the light into an Ando type AQ 1425 spectrum analyzer.

The transmission spectrum from a fiber without semiconductor cylinder is recorded first. Next, the transmission spectrum from a fiber with a semiconductor cylinder is recorded. The transmission spectrum from the fiber without semiconductor cylinder is used for normalizing the transmission spectrum data from the fibers with semiconductor cylinder.
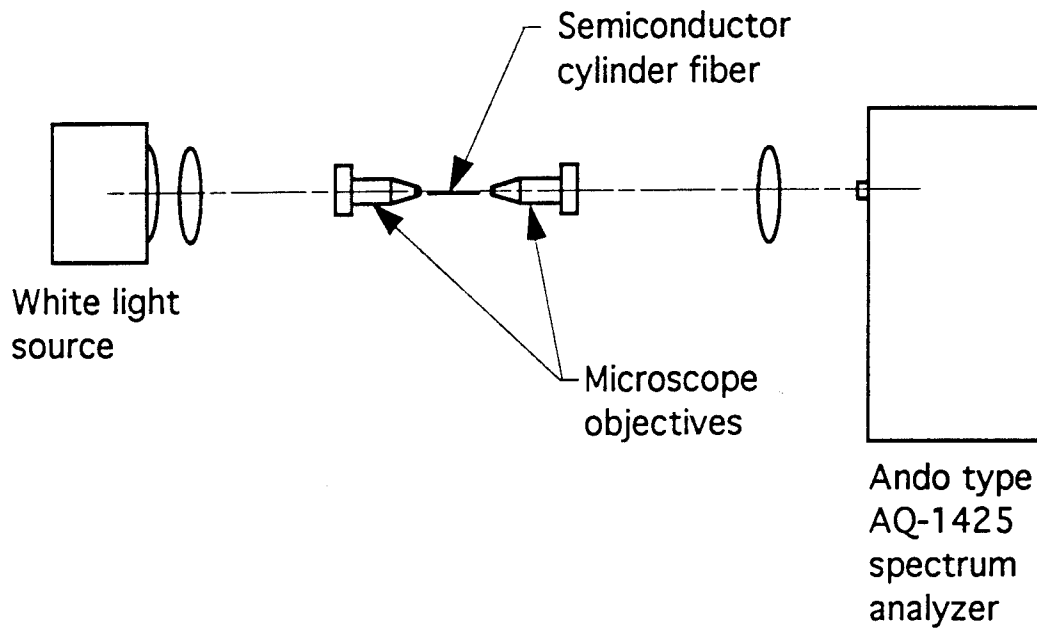
6

Fig. 5. Experimental set up for measuring the transmission spectrum of SCyFs.

2 THEORETICAL CALCULATIONS

Let us investigate the simplest possible case of light being guided in a QCyFLA. A cross section of this device is shown in Fig. 5. The TE mode is the simplest one to investigate. We approximate the thin semiconductor layer by a current sheet. The sheet conductivity σ of this layer is related to the imaginary part ε_I of the relative dielectric constant of the semiconductor layer.

$$\sigma = \frac{2\pi\varepsilon_I a}{c\lambda\mu_o}$$

$\qquad$ 1.1

where c is the velocity of light, λ is the wavelength, μ_o is the permeability of free space, and a is the thickness of the semiconductor cylinder.

The cylindrical coordinate system that we shall use is illustrated in Fig. 1. The light propagates in the z direction, the direction perpendicular to the plane of the cross section of the fiber. We assume, for simplicity,

that the electric field vector **E** of the light is in the θ direction, that it is independent of the angle θ, and that it has the form of a propagating wave.
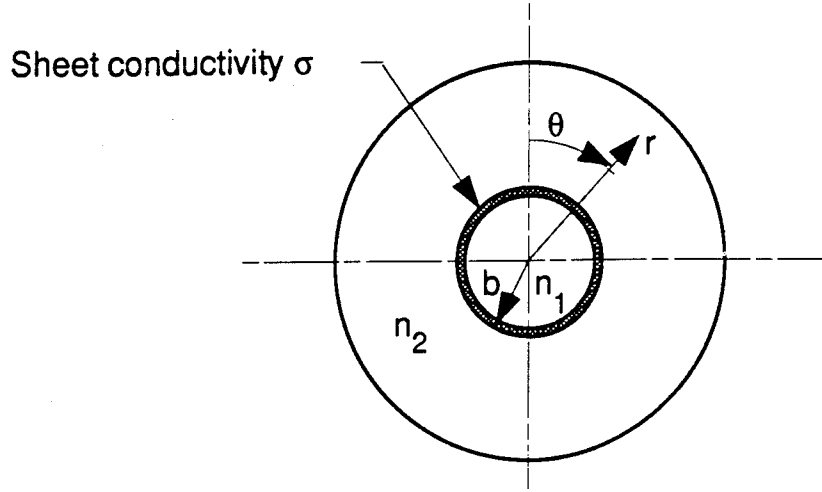

Fig. 5. Cross section of QCyFLA. The core has an index of refraction n_1 and the cladding has an index of refraction n_2. The semiconductor cylinder is represented by a conducting layer with a sheet conductivity σ.

$$\mathbf{E} = \hat{\mathbf{a}}_\theta E_\theta(r) e^{j(\omega t - kz)}$$ 1.2

The θ independent wave equation for a θ directed electric field E_θ in cylindrical coordinates is.

$$\frac{1}{r}\frac{\partial}{\partial r}\left[r\frac{\partial E_\theta(r)}{\partial r}\right] - \frac{E_\theta(r)}{r^2} - k^2 E_\theta(r) = \frac{n^2 \omega^2}{c^2} E_\theta(r)$$ 1.3

a) The Core

The electric field vector $\mathbf{E}_C$ in the core for the lowest order TE mode has only a θ directed component. The lowest order mode that is a solution of equation 1.3 is of the form:

$$E_C = \hat{a}_\theta E_C J_1(ur)e^{j(\omega t - kz))} \qquad 2.1$$

where $J_1(ur)$ is the first order Bessel function and k is the propagation constant of the electromagnetic wave. The dispersion relation of the light electromagnetic wave in the core can be obtained by substituting equation 2.1 into equation 1.3.

$$k^2 + u^2 = \frac{4\pi^2 n_1^2}{\lambda^2} \qquad 2.2$$

Let us assume the following form for the magnetic flux density vector $\mathbf{B}_C$ in the core:

$$\mathbf{B}_C = [\hat{a}_r B_{Cr}(r) + \hat{a}_z B_{Coz}J_0(ur)]e^{j(\omega t - kz)} \qquad 2.3$$

The zero order Bessel function $J_0(ur)$ is a solution of the θ independent wave equation in cylindrical coordinates of a z component.

We shall determine $B_{Cr}(r)$ and B_{Coz} from Maxwell's equations. The Ampere-Maxwell equation is:

$$\nabla \times \mathbf{B}_C = \frac{n_1^2 \omega}{c^2} \mathbf{E}_C \qquad 2.4$$

From the θ component of the Ampere-Maxwell equation we have:

$$- jkB_{Cr}(r) + B_{Coz}J_1(ur) = j\frac{n_1^2 \omega}{c^2}E_C J_1(ur) \qquad 2.5$$

where we have made use in equation 2.5 of the fact that:

$$\frac{dJ_0(ur)}{dr} = - uJ_1(ur) \qquad 2.6$$

The Faraday-Maxwell equation is:

$$\nabla \times \mathbf{E} + j\omega\mathbf{B} = 0 \qquad\qquad 2.7$$

We have from the Faraday-Maxwell equation for the r component:

$$jkE_C J_1(ur) + j\omega B_{Br}(r) = 0 \qquad\qquad 2.8$$

and for the z component

$$E_C\frac{1}{r}\frac{\partial}{\partial r}[rJ_1(ur)] + j\omega B_{Coz}J_0(ur) = 0 \qquad\qquad 2.9$$

By differentiating equation 2.8 with respect to r we obtain:

$$E_C\frac{1}{r}\frac{\partial}{\partial r}\left[r\frac{\partial J_1(ur)}{\partial r}\right] - E_C\frac{J_1(ur)}{r^2} - j\omega B_{Coz}J_1(ur) = 0 \qquad\qquad 2.10$$

where we made use of equation 2.6 in equation 2.10. By performing the differentiations in equation 2.10 we obtain:

$$[E_C u^2 - j\omega u B_{Coz}]J_1(ur) = 0 \qquad\qquad 2.11$$

From equation 2.8 and 2.11 into equation 2.3 we obtain for the magnetic flux density vector in the core:

$$\mathbf{B}_C = -\left[\hat{\mathbf{a}}_r\frac{k}{\omega}J_1(ur) + j\hat{\mathbf{a}}_z\frac{u}{\omega}J_0(ur)\right]E_C e^{j(\omega t - kz)} \qquad\qquad 2.12$$

The electric field vector has only a component that is transverse to the propagation of the electromagnetic field while the magnetic flux density vector has components both perpendicular and in the direction of propagation of the electromagnetic field. We have not used equation 2.5 in our derivation. However, by substituting equation 2.8 into equation 2.5 and

making use of equation 2.2 we obtain a result that is identical to equation 2.11.

b) The Cladding

The electric field vector $\mathbf{E}_D$ in the cladding of the TE mode has, also, only a θ directed component. The lowest order mode that is a solution of equation 1.3 is of the form:

$$\mathbf{E}_D = \hat{a}_\theta E_D K_1(wr)e^{j(\omega t - kz))} \qquad 3.1$$

where $K_1(wr)$ is the first order modified Bessel function. The function $K_1(wr)$ decays monotonically to zero for large r. The dispersion relation of the light electromagnetic wave in the cladding can be obtained by substituting equation 3.1 into equation 1.3.

$$k^2 - w^2 = \frac{4\pi^2 n_2^2}{\lambda^2} \qquad 3.2$$

By using a method similar to the one leading to equations 3.2 we obtain for the components of the magnetic flux density vector $\mathbf{B}_D$ in the cladding:

$$\mathbf{B}_D = -\left[\hat{a}_r \frac{k}{\omega}K_1(wr) - j\hat{a}_z \frac{w}{\omega}K_o(wr)\right]E_D e^{j(\omega t - kz)} \qquad 3.3$$

where we made use of the fact that:

$$\frac{dK_o(wr)}{dr} = -wK_1(wr) \qquad 3.4$$

c) Boundary Conditions

The thin semiconductor notwithstanding the tangential components of the electric field vector are continuous across the core cladding boundary.

From Fig. 1 we observe that the core has a radius b. Therefore, at r = b the θ components of the electric field vectors in the core and cladding are equal.

$$E_C J_1(ub) = E_D K_1(wb) \qquad 4.1$$

The normal components of the magnetic flux density vector are continuous across the core cladding boundary. Therefore, at r = b the r components of the magnetic flux density vector in the core and cladding are equal.

$$-\frac{k}{\omega} E_C J_1(ub) = -\frac{k}{\omega} E_D K_1(wb) \qquad 4.2$$

Equation 4.2 is essentially identical to equation 4.1 and, thus, does not provide any new information. The difference between the tangential components of the magnetic flux density vectors in the cladding and core are equal to the surface current density in the semiconductor layer times the permeability of free space.

$$\hat{a}_z \cdot B_C(b) - \hat{a}_z \cdot B_D(b) = \mu_0 \sigma \hat{a}_\theta \cdot E_D(b) \qquad 4.3$$

By substituting the z components of equations 2.12 and 3.3 and equation 3.1 into equation 4.3 we obtain:

$$- j\frac{u}{\omega} E_C J_0(ub) - j\frac{w}{\omega} E_D K_0(wb) = \mu_0 \sigma E_D K_1(wb) \qquad 4.4$$

By collecting terms in equation 4.4 we obtain:

$$- u E_C J_0(ub) = [j\omega\mu_0 \sigma K_1(wb) + w K_0(wb)] E_D \qquad 4.5$$

By dividing equation 4.5 by equation 4.1 and substituting equation 1.1 into the resulting expression for σ we obtain:

$$\frac{uJ_0(ub)}{J_1(ub)} + j\frac{4\pi^2\varepsilon_I a}{\lambda^2} + \frac{wK_0(wb)}{K_1(wb)} = 0 \qquad 4.6$$

Equation 4.6 together with equations 2.2 and 3.2 constitute the dispersion relation of this TE mode in the QCyFLA. For ε_I equal to zero equation 4.6 is identical to the equation for the TE mode of a step index fiber as derived in the literature.

d) The Gain Coefficient

We will, next, calculate the imaginary part of the propagation constant. Since the propagation constant has a real and imaginary part from equations 2.2 3.2 that both u and w must also have real and imaginary parts. To this end we let:

$$k \equiv \beta + j\alpha, \qquad u \equiv u_0 + j\eta, \qquad \text{and} \qquad w \equiv w_0 + j\theta \qquad 5.1$$

By expanding equation 4.6 to first order in the small imaginary parts of u and w we obtain:

$$\frac{u_0 J_0(u_0 b)}{J_1(u_0 b)} + \frac{w_0 K_0(w_0 b)}{K_1(w_0 b)} + j\frac{4\pi^2\varepsilon_I a}{\lambda^2} - ju_0 b\left[1 - \frac{J_0^2(u_0 b)}{J_1^2(u_0 b)}\right]\eta -$$

$$jw_0 b\left[1 - \frac{K_0^2(w_0 b)}{K_1^2(w_0 b)}\right]\theta = 0 \qquad 5.2$$

By substituting equations 5.1 into equations 2.2 and 3.2 we obtain for the real parts of the dispersion relations in the core and cladding respectively:

$$\text{a) } \beta^2 + u_0^2 \approx \frac{4\pi^2 n_1^2}{\lambda^2} \qquad \text{and} \qquad \text{b) } \beta^2 - w_0^2 \approx \frac{4\pi^2 n_2^2}{\lambda^2} \qquad 5.3$$

13

where we neglected the terms α^2, η^2, and θ^2 since α η and θ are typical equal to a few reciprocal mm while u_o and w_o are equal to a few reciprocal μm and ß is of the order of a reciprocal light wave length long. Similarly, we obtain for the imaginary parts of the dispersion relations in the core and cladding respectively:

a) $\beta\alpha + u_o\eta = 0$ and b) $\beta\alpha - w_o\theta = 0$ 5.4

By collecting real terms of equation 5.2 we obtain:

$$\frac{u_o J_0(u_o b)}{J_1(u_o b)} + \frac{w_o K_0(w_o b)}{K_1(w_o b)} = 0 \qquad 5.5$$

We, next, collect the imaginary parts of equation 5.2 and substitute equations 5.4 for η and θ.

$$\alpha\beta b \left[\frac{J_0^2(u_o b)}{J_1^2(u_o b)} - \frac{K_0^2(w_o b)}{K_1^2(w_o b)} \right] = \frac{4\pi^2 \varepsilon_I a}{\lambda^2} \qquad 5.6$$

Equation 5.6 can be solved for the gain coefficient α:

$$\alpha = \frac{4\pi^2 \varepsilon_I a}{\lambda^2 b\beta} \left[\frac{J_0^2(u_o b)}{J_1^2(u_o b)} - \frac{K_0^2(w_o b)}{K_1^2(w_o b)} \right]^{-1} \qquad 5.7$$

where ß, u_o, and w_o can be determined from equations 5.3 and 5.5. By substituting equation 5.5 for $\dfrac{K_0(w_o b)}{K_1(w_o b)}$ and substituting equations for u_o^2 and w_o^2 into the resulting expression we obtain:

14

$$\alpha = \frac{\beta^2 \dfrac{\lambda^2}{4\pi^2} - n_2^2}{\beta^2 \dfrac{\lambda^2}{4\pi^2} - \dfrac{n_1^2 + n_2^2}{2}} \; \frac{J_1^2(u_ob)}{J_0^2(u_ob)} \; \frac{2\pi^2 \varepsilon_I a}{\lambda^2 \beta b} \qquad\qquad 5.8$$
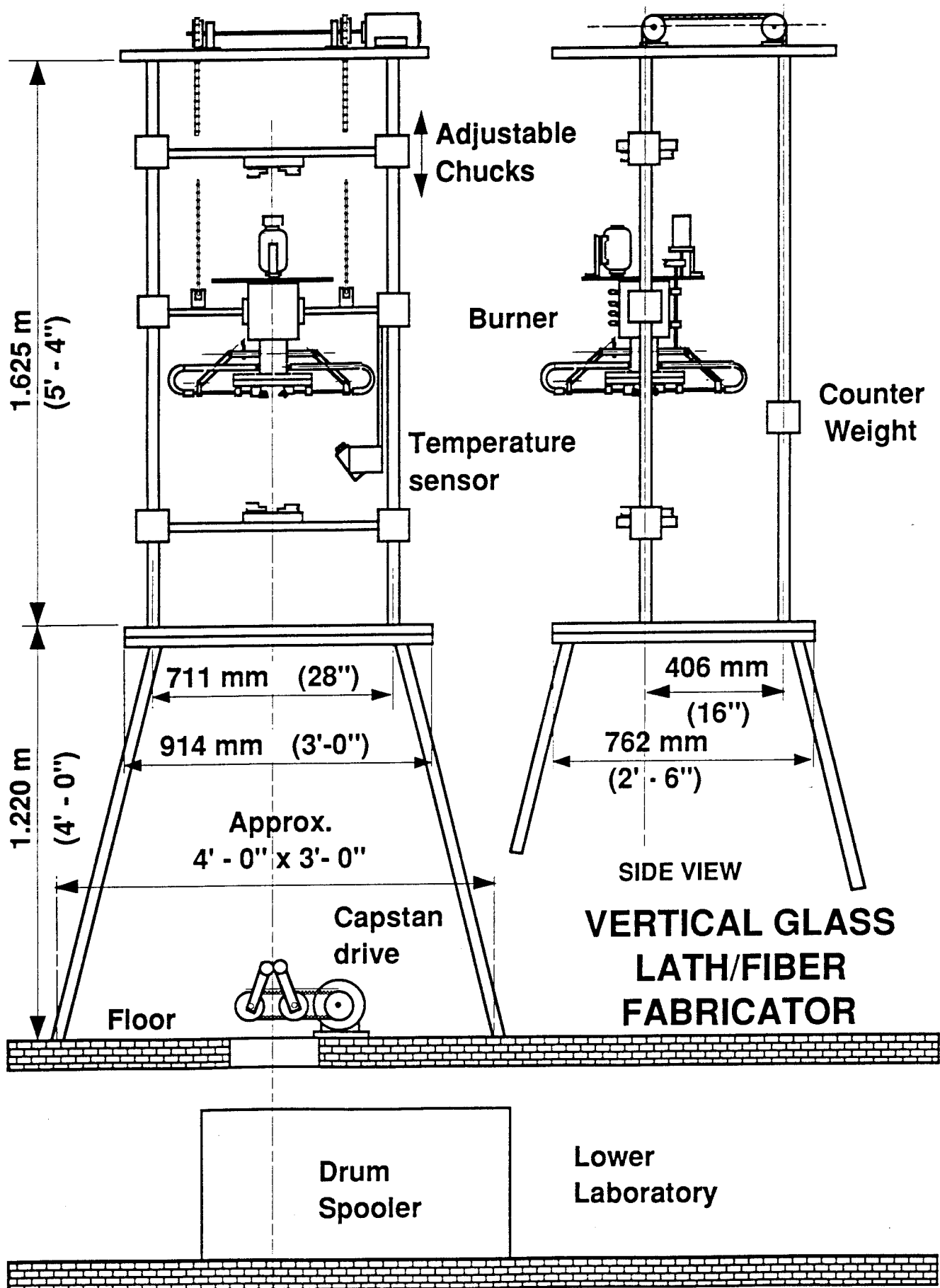
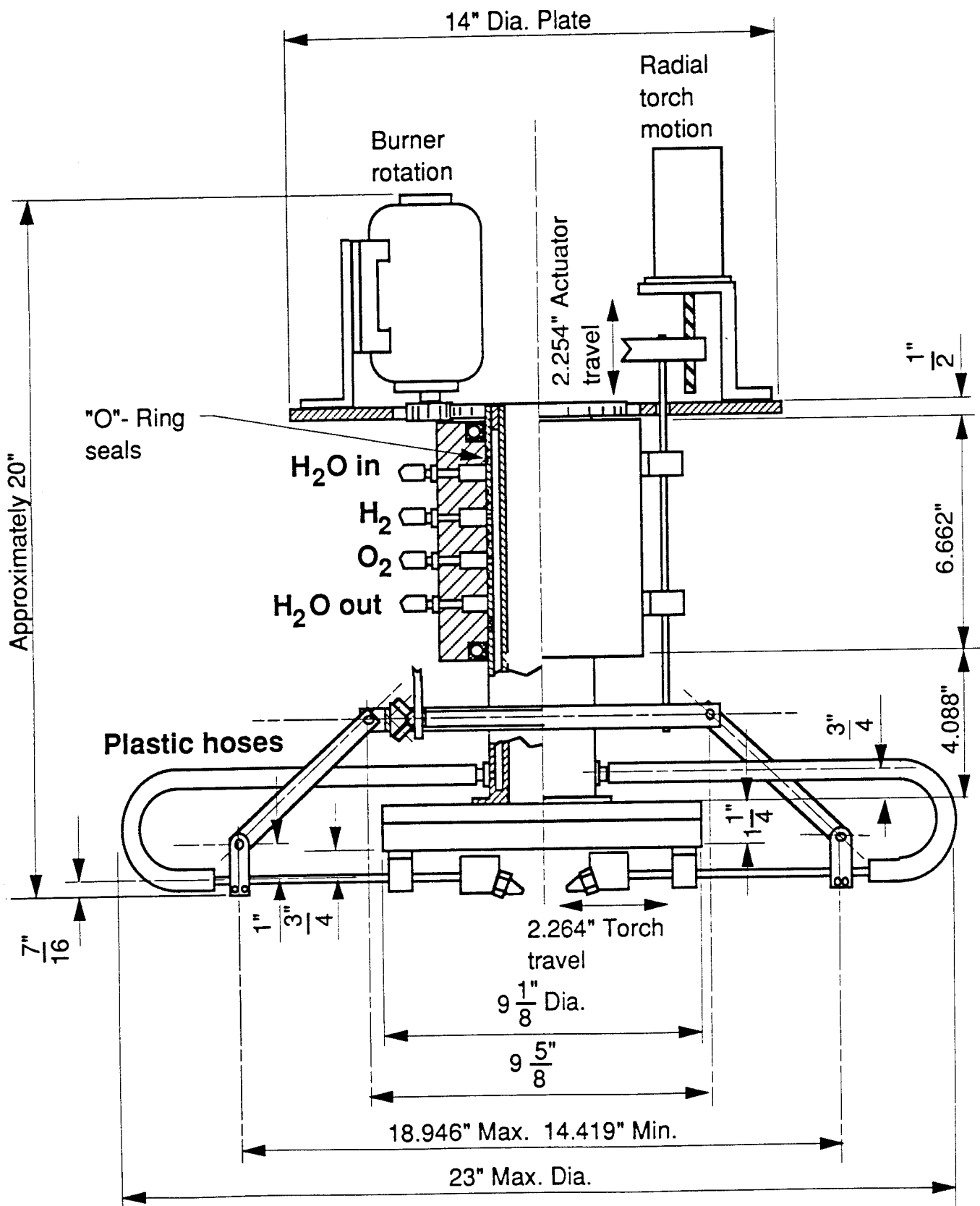Since both u_o and w_o must be real we observe from equations 5.3 that:

$$n_2^2 \le \beta^2 \frac{\lambda^2}{4\pi^2} \le n_1^2 \qquad\qquad 5.9$$

3 NEW VERTICAL GLASS LATH/FIBER PULLING EQUIPMENT AND NEW VACUUM SYSTEM

We and have currently in operation a computer controlled vertical glass lath/fiber pulling tower. Our current equipment has several drawbacks: The glass has to rotate instead of the burner rotating and the burner temperature is controlled by controlling the gas flow to the burner nozzles. Some times, when decreasing the gas flow to the burner nozzles the burner would go out. This often happens with welding torches under similar conditions.

We designed, and have currently under constructed a new vertical glass lath/fiber pulling tower. This equipment is two floors tall, see Fig. 6. The new burner which is nearing completion, has been tested and it does rotate. The new burner has 8 torches each of which can be moved 2.25 inches radially while the burner is rotating, see Fig. 7. Thus, one can use the torch position to control the glass temperature. Also, the variation of the radial torch position greatly increases the flexibility of the glass lath.

Adjustable Chucks

1.625 m (5' - 4")

Burner

Temperature sensor

Counter Weight

711 mm (28")

406 mm (16")

914 mm (3'-0")

762 mm (2' - 6")

1.220 m (4' - 0")

Approx. 4' - 0" x 3'- 0"

SIDE VIEW

Capstan drive

VERTICAL GLASS LATH/FIBER FABRICATOR

Floor

Drum Spooler

Lower Laboratory

BURNER

We have several diffusion furnaces that will be used for curing the semiconductor films.

The method of fabricating QCyFLAs we are proposing is as follows: We vacuum deposit the semiconductor films on an optically quality glass rod. We plan, at first, to use 4 mm diameter Corning type 7059 Baria Aluminum Borosilicate glass rods with a coefficient of expansion α of 45 x 10^{-7}, a softening point of 720°C, and an index of refraction n_0 of 1.550. 10 mm O. D. and 6 mm I. D. Corning type 7052 Alcali Borosilcatete glass tubes with a coefficient of expansion α of 51.1 x 10^{-7}, a softening point of 718°C, and an index of refraction n_0 of 1.486 will be used for the cladding. InAs is deposited by using temperature controlled InAs and As effusion cells, and CdS is deposited by using temperature controlled CdS and S effusion cells. The glass rod is rotated at about 30 RPM during the deposition. The substrate is heated by tubular radiation heaters to about 500°C. for both semiconductors. This will probably be varied to maximize the film qualities. For example, at 500°C neither In which melts at 156°C nor As which sublimes at 358°C will deposit. However, InAs which melts at 935°C will deposit. The vacuum deposited semiconductor film are, usually, of poor quality. Therefore, we plan to cure the semiconductor film in a diffusion furnace by circulating HCl saturated N_2 gas, first, over semiconductor powder and than over the vacuum deposited film. This process restores the stochimetry of the film. We have, successfully used this technique previously in fabricating high quality CdS photoconducting films.

The semiconductor coated glass rod is, next, inserted in to the glass tube that will form the cladding. The glass tube is sealed at the top. The glass tube is repeatedly evacuated and flushed with N_2 gas. The tube is, finally, evacuated and back filled with N_2 gas to a pressure of about 2 mTorr and sealed. The burner will be used to collapse the tube onto the rod trapping the semiconductor film. The tube is clamped by chucks both ends. Since no elongation of the tube and rod occurs in this process the total cross sectional area of both the semiconductor film and the glass structure is preserved in this process. The structure has a cross sectional area of 6.2958 x 10^{-5} m^2 at this point in the process.

The apparatus will, finally, be used to pull a 120 µm diameter fiber from the preform. Considerable elongation of the glass and semiconductor

film occurs in this process. However, the proportionality of all radial dimensions are preserved. The fiber pulling process should result in a 50 Å thick semiconductor film surrounding a 30 μm diameter glass core.

Rome Laboratory

Customer Satisfaction Survey

RL-TR-_____

Please complete this survey, and mail to RL/IMPS,
26 Electronic Pky, Griffiss AFB NY 13441-4514. Your assessment and
feedback regarding this technical report will allow Rome Laboratory
to have a vehicle to continuously improve our methods of research,
publication, and customer satisfaction. Your assistance is greatly
appreciated.
Thank You

_____

_____

Organization Name:_____(Optional)

Organization POC: _____(Optional)

Address:_____

1.   On a scale of 1 to 5 how would you rate the technology
developed under this research?

     5-Extremely Useful   1-Not Useful/Wasteful

                    Rating_____

Please use the space below to comment on your rating. Please
suggest improvements. Use the back of this sheet if necessary.

2.   Do any specific areas of the report stand out as exceptional?

                    Yes____ No_____

     If yes, please identify the area(s), and comment on what
aspects make them "stand out."

3. Do any specific areas of the report stand out as inferior?

<div align="center">Yes____   No____</div>

    If yes, please identify the area(s), and comment on what aspects make them "stand out."

4. Please utilize the space below to comment on any other aspects of the report. Comments on both technical content and reporting format are desired.

MISSION

OF

ROME LABORATORY

Mission. The mission of Rome Laboratory is to advance the science and technologies of command, control, communications and intelligence and to transition them into systems to meet customer needs. To achieve this, Rome Lab:

    a. Conducts vigorous research, development and test programs in all applicable technologies;

    b. Transitions technology to current and future systems to improve operational capability, readiness, and supportability;

    c. Provides a full range of technical support to Air Force Materiel Command product centers and other Air Force organizations;

    d. Promotes transfer of technology to the private sector;

    e. Maintains leading edge technological expertise in the areas of surveillance, communications, command and control, intelligence, reliability science, electro-magnetic technology, photonics, signal processing, and computational science.

The thrust areas of technical competence include: Surveillance, Communications, Command and Control, Intelligence, Signal Processing, Computer Science and Technology, Electromagnetic Technology, Photonics and Reliability Sciences.